Int. J. Electrochem. Sci., 9 **(2014)** 7287 - 7299

International Journal of
ELECTROCHEMICAL
SCIENCE
www.electrochemsci.org

Mechanism of GaAs Surface Sulfidation

M. J. Al Marri[1], *E. M. Fayyad*[2,3], *A. Hassan*[1,4], *M. M. Khader*[1,*]

[1] Gas Processing Center, College of Engineering, Qatar University, Doha P.O. Box 2713, Qatar,
[2] Physical Chemistry Department, National Research Center, Dokki, Giza 12311, Egypt
[3] Center for Advanced Materials, Qatar University, Doha P.O. 2713
[4] Chemistry Department, Faculty of Science, Alexandria University, Alexandria, Egypt.
[*]E-mail: mmkhader@qu.edu.qa

Received: 23 August 2014 / *Accepted:* 20 September 2014 / *Published:* 29 September 2014

The mechanism of GaAs sulfidation under illumination and potentiodynamic polarization was investigated in acidified thiourea (TU) electrolytes. Sulfidation generated smooth surfaces, as revealed by scanning electron microscopy and atomic force microscopy images; but analysis by inductively coupled plasma – mass spectroscopy (ICP-MS) of spent electrolytes showed that this was in part due to GaAs dissolution. The initial step in sulfidation occurred through formation of elemental arsenic which then reacted with TU and forms As(III) sulfide, which was subsequently oxidized into As(V) sulfide and finally to arsenic sulfate. X- Ray photoelectron spectroscopy (XPS) demonstrated the initial formation of elemental As (XPS peak at 42 eV of As – As bond). XPS also showed three S 2p doublets at 162.4 eV which were assigned to (As(III) – S), 164.4 eV for (As(V) – S) and 169.1 eV for (S – O). The intensity of the XPS peak due to As(V) – S (S 2p at 164.4 eV) increased with prolonged exposure to sulfidation by the electrolyte, indicating the oxidation of As(III) into As(V) sulfide. Furthermore, the intensity of the S – O bond (S 2p at 169.1 eV) decreased with time, presumably due to arsenic sulfate dissolution. Both XPS and ICP-MS studies revealed that arsenic species were preferentially segregated on the surface but Ga ions diffused towards the electrode bulk.

Keywords: GaAs, Arsenic sulfide, X- Ray photoelectron spectroscopy, Atomic force microscopy, Corrosion inhibition.

1. INTRODUCTION

GaAs surface passivation is an important objective for application in fabricating electronic devices. This passivation has been achieved by various methods, including formation of thin surface layers of either sulfide [1, 2], selenide [3 – 5] or noble metals [6 – 8]. These have been incorporated on the GaAs surface by diverse methods, including electroless [10], electrochemical [11, 12],

photochemical [13] and gas phase deposition processes [14]. Sulfidation of GaAs is of particular interest for corrosion inhibition [1, 2, 9 – 11]; and various sulfur-containing compounds have been investigated for this application, including sodium sulfide [1, 10, 11], ammonium sulfide [14 – 16], sulfur chloride [17], thiols [18] and other complex organic compounds [19, 20]. The formation of sulfides during aqueous electrochemical deposition is accompanied by the formation of oxide species [21]. Usually, this oxidation is not uniform and a variety of different oxide species are formed on the GaAs surface [22 – 24].

In past work, we reported that the electrochemical behavior of n-GaAs in acidified thiourea electrolytes resulted in the formation of an As-sulfide surface [25]. The aim of the present research is to gain more insight into the mechanism of GaAs sulfidation.

2. EXPERIMENTAL

2.1. Electrode preparation

Silicon-doped n-GaAs wafers with a doping density of $2x10^{16}$ cm^{-3} were purchased from MCP Ltd. The wafers were attached to an aluminum holder (a cylinder of 10 mm diameter and 2 mm thickness) using silver epoxy to establish electrical contact. The aluminum holder was then threaded into a 12-cm long, 2.5 mm diameter aluminum rod which served both as a support for the working electrode and as a current lead. The exposed surface area of GaAs to the electrolyte was 19.6 mm^2. The aluminum holder and the part of the aluminum rod that was exposed to electrolyte were insulated by covering them in a paraffin film, which was in turn covered with a layer of araldite. After carrying out electrochemical measurements on the GaAs sample, the GaAs sample was removed for Atomic Force Microscopy (AFM), Scanning Electron Microscope (SEM) and X- Ray photoelectron Spectroscopy (XPS) investigations. Using this arrangement there was no need for physical contact with the GaAs sample following the electrochemical cycles, prior to AFM, SEM and XPS measurements.

2.2. Electrochemical deposition of sulfide film

The electrochemical measurements on freshly etched samples were carried out in a three-electrode electrochemical cell with GaAs serving as the working electrode, Ag/AgCl as the reference electrode and a Pt wire as the counter electrode. The GaAs electrode was cleaned by etching in a mixture of 30% H_2O_2, 6 M H_2SO_4 and H_2O (1:1:1 volume) for 5 min. The electrode was illuminated by a 150 W xenon arc lamp. Light was filtered from UV and IR by 420 nm and water cut-off filters. The light intensity was measured using an Eppley thermopile. Arsenic sulfide was deposited electrochemically under illumination with light intensity of 25 mW cm^{-2}, in electrolytic mixtures of thiourea (TU) and H_2SO_4 of various concentrations. The GaAs electrodes were subjected to continuous scanning from -1 to +1 V vs. Ag/AgCl at a scan rate of 20 mV s^{-1}. All reagents were analytical grade. All potentials were measured versus Ag/AgCl.

2.3. Electrochemical oxidation of GaAs

Oxidation of the sample was carried out in a 10% H_2O_2 solution, acidified with 0.1 M H_2SO_4. As with sulfidation, oxidation was also carried out under potentiodynamic control with constant illumination.

2.4. Scanning electron microscopy SEM:

The surface microstructure and morphology were studied using a JEOL 840A SEM. The SEM accelerating voltage was 1,000 volts to 40,000 volts with an increment of 1,000 volts.

2.5. Atomic force microscopy (AFM):

GaAs surface topography was investigated using an atomic force microscope to determine the effect of electrochemical treatment on surface roughness. A MFP3D Asylum research 6310 AFM was used for this study. The AFM was operated in contact mode in air at room temperature. It was operated in the low-voltage mode to minimize electronic noise, with a contact force (between cantilever and sample) of approximately 10^{-9} N. A 5 μm scan width was used to obtain the images. The probes were made of non-conductive silicon nitride with a nominal cantilever spring constant of 0.01 N/m. SEM images were taken before and after the AFM investigation. These images did not show significant scratching on the GaAs samples due to contacting with the AFM silicon nitride probe. The variation in surface roughness of the samples is visualized in height images showing as bright and dark regions on the surface, representing peaks and valleys respectively. Surface roughness and standard deviation values of the samples were obtained and analyzed.

2.6. Analysis of dissolved As and Ga ions

The amounts of dissolved arsenic and gallium ions in the spent electrolytes were determined quantitatively by inductively coupled plasma-mass spectrometry (ICP-MS) (Agilent, 7500Ce), which utilized an octapole ion guide enclosed in a collision/reaction cell.

2.7. X-ray photo-electron spectroscopy (XPS)

All XPS spectra were taken on a Kratos Axis-Ultra DLD spectrometer. The X-ray analysis area for these acquisitions was approximately 300x700 μm. Monochromatic Al Ka X-rays (1486.6 eV) were used as the excitation source and a pressure of $6.5x10^{-7}$ Pa was maintained in the spectrometer chamber. An accelerating voltage of 15 kV and an anode current of 15 mA were employed during analyses. The spectrometer pass energy for survey spectra (to calculate composition) was 80 eV and the pass energy for high resolution scans was 20 eV. The take-off

angle (the angle between the sample normal and the input axis of the energy analyzer) was 0º, and the input lens was operated in hybrid mode (0º take-off angle 100 Å sampling depth).

Casa XPS analysis software was used to determine peak areas, to calculate the elemental compositions from peak areas above a linear background, and to peak fit the high resolution spectra. The binding energy scales for the high-resolution spectra were calibrated by assigning the most intense C1s high-resolution peak a binding energy of 285.0 eV. Peak fits of S2p, Ga3d, and As3d doublets were constrained so that the (3/2, 1/2) and (5/2, 3/2) doublet peaks had the same full width at half maximum (FWHM). Three spots were analyzed on each sample. Analysis of the samples included survey spectra of all three spots, and high resolution spectra from one spot. High resolution spectra were obtained for the C1s, S2p, Ga3d and As3d peaks. Samples were cleaned by rinsing for few minutes in acetone followed by methanol. All sample handling was done with tools that were twice cleaned by solvents; the solvents were HPLC-grade. For surface cleaning, before carrying out XPS experiments, all samples were sputtered for 10 minutes by Ar ions. Some samples were sputtered for longer times to do the XPS depth profiling investigation. Sputter-etching was performed with a Kratos ion gun using 5keV argon ions electronically rastered over a 2x2 mm area. The gun was operated in the beam monitor current controlled mode, with a monitor current of 159 nA.

3. RESULTS & DISCUSSION

3.1. Scanning electron microscopy and atomic force microscopy:

GaAs surface morphology was investigated by SEM and AFM after treatment in 0.8 M TU electrolytes acidified with H_2SO_4 in concentrations varying from 0.1 M to 0.5 M. In all cases, it was observed that exposure of GaAs electrodes to TU solution acidified by high H_2SO_4 concentrations resulted in the formation of smooth surfaces, which may be attributed to corrosion inhibition. Lower H_2SO_4 concentrations resulted in rougher surfaces. Examples of SEM and AFM micrographs after exposure to TU electrolyte in two different H_2SO_4 concentrations are shown in Fig. 1 and 2, respectively. It was observed that exposure to a high concentration of H_2SO_4 formed a shiny golden layer of As-sulfide [25]. The SEM micrographs (Fig. 1) clearly show the effect of acid concentration on surface smoothness: in 0.5M H_2SO_4 the surface is obviously smoother than in 0.1 M solution. This is further quantified by the AFM results. Fig. 2 displays the AFM 2D topography images and roughness surface analysis of sulfidized GaAs in a mixture of 0.8 M TU acidified by 0.5 M H_2SO_4 (Fig. 2a) and 0.1 M H_2SO_4 (Fig. 2b). The mean surface roughness parameter (R_a) and average standard deviation values for these samples are presented in Table 1. The images clearly reveal the smoother surface generated at higher acid concentration. The average surface roughness of GaAs decreased from 100.1 nm in 0.1 M H_2SO_4 to 34.8 nm when generated in 0.5 M H_2SO_4. This large variation in surface roughness observed between GaAs samples is similar to the results obtained by SEM. The decrease in the R_a value also is a clear indication of the smoother surface obtained at higher acid concentration.

Table 1. Effect of H_2SO_4 concentration on surface roughness: Atomic force microscopy results:

Samples	Mean surface roughness (R_a)	Standard deviation (SD)
Sample 1[a)]	34.805 nm	10.117 nm
Sample 2[b)]	100.117 nm	19.037 nm

GaAs was sulfidized under potentiodynamic scanning for 25 scans from – 1 to + 1 V at 20 mV s^{-1} under illumination by light of intensity 25 mW cm^{-2} in a mixture of 0.8 M TU (a) 0.5 M H_2SO_4 and (b) 0.1 M H_2SO_4**.**

Another important indication of corrosion inhibition due to sulfidation in higher H_2SO_4 acid concentrations can be deduced from the ICP-MS results shown in Fig. 3. This figure also shows preferential arsenic dissolution at all acid concentrations.

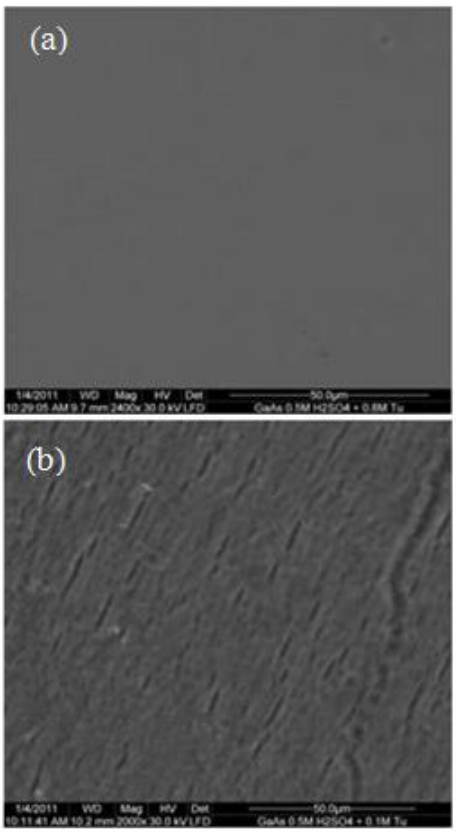

Figure 1. Scanning electron micrographs of GaAs after potentiodynamic scanning for 25 scans from – 1 to + 1 V at 20 mV s^{-1} under illumination by light of intensity 25 mW cm^{-2}. The electrolytes were made of 0.8 M TU mixed with: a) 0.5 M H_2SO_4 and b) 0.1 M H_2SO_4.

The formation of surface sulfide at higher acid concentrations could be accounted for by two effects: 1) the stripping oxide layers from the GaAs surface prior to sulfide deposition, as reported earlier [21, 22], and 2) protonation of the TU molecules in accordance to following equation [26 – 28]:

$$(NH_2)_2CS + 2H^+ \rightleftharpoons [(NH_3)_2CS]^{+2} \quad (1)$$

This reaction has a pK value of -1.44 at 298 K [27], with K being the protonation constant. Accordingly, at higher acid concentration, because of protonation of the TU amine groups, adsorption on the GaAs surface via TU nitrogen atoms is not favored. Thus, TU adsorption is expected to occur via the sulfur atoms on the GaAs surface. The following mechanism for the adsorption and electro-oxidation of TU on GaAs surface is therefore proposed:

$$GaAs + 3h^+ \rightarrow As + Ga^{3+} \quad (2)$$

$$As + [(NH_3)_2CS]^{+2} \rightarrow As[(NH_3)_2CS]^{2+\cdot} + h^+ \quad (3)$$

$$2As[(NH_3)_2CS]^{2+\cdot} \longrightarrow As(NH_3)_2^{2+}C - S - S - C(NH_3)_2^{2+}As \quad (4)$$

$$As(NH_3)_2^{2+}C - S - S - C(NH_3)_2^{2+}As + 2H_2O + 4h^+ \rightleftharpoons [As_2S_2]^* + 2(NH_2)_2CO + 8H^+ \quad (5)$$

$$3[As_2S_2]^* + 6h^+ \longrightarrow 2As_2S_3 + 2As^{+3} \quad (6)$$

$$As_2S_3 + [As_2S_2]^* \longrightarrow As_2S_5 + 2\,As \quad (7)$$

$$As_2S_3 + 12H_2O + 24h^+ \longrightarrow As_2(SO_4)_3 + 4H^+ \quad (8)$$

Reaction (2) corresponds to the initial photoelectrochemical oxidation of GaAs, forming elemental surface arsenic.

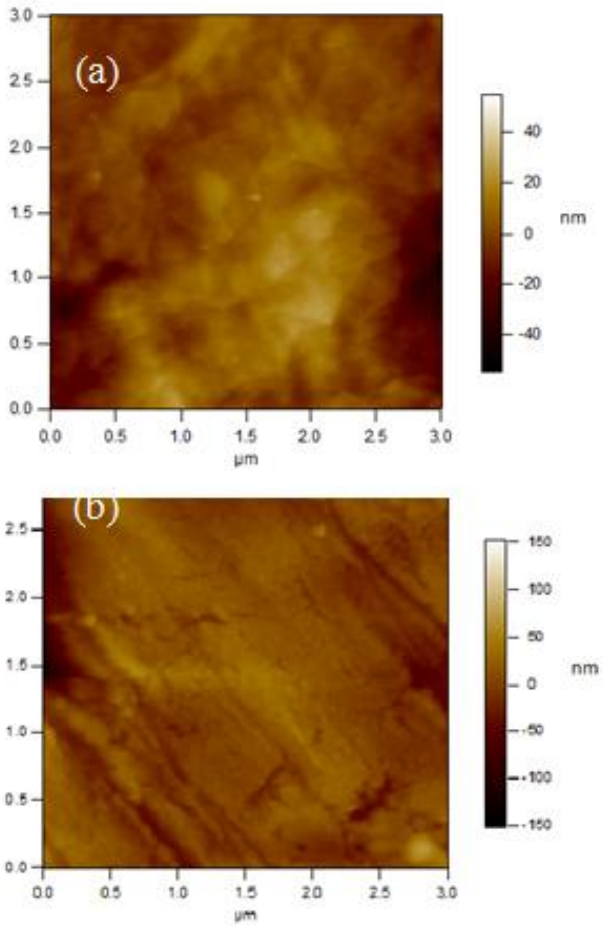

Figure 2. 2D atomic force microscopy topography images of GaAs sulfidized under potentiodynamic scanning for 25 scans from – 1 to + 1 V at 20 mV s^{-1} under illumination by light of intensity 25 mW cm^{-2} in a mixture of 0.8 M TU (a) 0.5 M H_2SO_4, and (b) 0.1 M H_2SO_4).

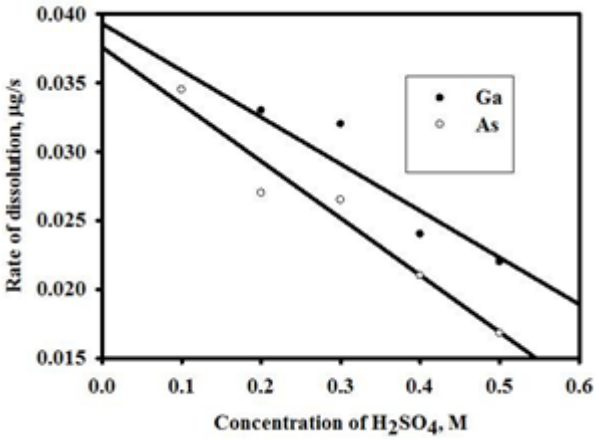

Figure 3. Results of inductively coupled plasma – mass spectroscopy analysis of spent electrolytes; the electrode was scanned 50 times under illumination in an electrolyte made of: a) 0.8 M TU acidified by H_2SO_4 of various concentrations.

Reaction (3) is the photoelectrochemical - oxidation of thiourea adsorbate yielding the radical ion through a single electron transfer. Reaction (4) represents the fast formation of formamidine disulphide on the GaAs surface. Reaction (5) represents the aqueous hydrolysis of formamidine disulphide into an arsenic sulfide intermediate, $[As_2S_2]^*$ and urea. This intermediate is the sulfur supplying component of the GaAs sulfidation process. Reaction (6) corresponds to the photoelectrochemical oxidation of the intermediate to As(III)sulfide. Reaction (7) is the subsequent photoelectrochemical oxidation of As(III)sulfide into As(V)sulfide. Finally, reaction (8) corresponds to the photoelectrochemical oxidation of As(III)sulfide into As(III)sulfate. It is unlikely to from As(V)sulfate as this compound might not exist but As(V)sulfide and As(III)sulfate are known arsenic compounds [29, 30].

The above proposed mechanism is supported by the experimental results as presented in the discussion below.

3.2. XPS analysis

Table 2. Surface Chemical Bonding

GaAs	Peak	corrected BE, eV	Assignment	FWHM	% of element
Untreated	C 1s	285.0	C-C,H	1.0	100.0
	Ga 3d5/2	18.9	Ga-As	0.7	71.7
	Ga 3d5/2	20.0	Ga-O	1.0	28.3
	As 3d5/2	41.5	As-Ga	0.8	80.9
	As 3d5/2	44.5	As-O	1.8	19.1
Sulfuric acid	C 1s	285.0	C-C,H	1.0	100.0
	Ga 3d5/2	18.9	Ga-As	0.6	67.7
	Ga 3d5/2	20.0	Ga-O	1.0	32.3
	As 3d5/2	40.8	As-Ga	1.6	60.2
	As 3d5/2	43.9	As-O	2.3	39.8

Short time sulfidized	C 1s	285.0	C-C,H	1.2	49.4
	C 1s	288.3	C=O	1.6	32.4
	C 1s	285.7	C-N	1.2	18.2
	S 2p3/2	162.4	Sulfide-"As(III)"	1.2	40.8
	S 2p3/2	169.1	S-O	1.4	46.7
	S 2p3/2	164.3	Sulfide-"As(V)"	1.2	12.5
	As 3d5/2	41.8	As-As	0.8	49.2
	As 3d5/2	42.6	As-S	0.8	50.8
Long time sulfidized	C 1s	285.0	C-C,H	1.4	49.9
	C 1s	288.4	C=O C-	1.4	28.1
	C 1s	286.2	N	1.4	22.0
	S 2p3/2	162.3	Sulfide-"As(III)"	1.0	46.3
	S 2p3/2	168.6	S-O	1.2	18.2
	S 2p3/2	163.7	Sulfide-"As(V)"	1.4	35.5
	As 3d5/2	42.0	As-As	1.1	66.6
	As 3d5/2	42.5	As-S	1.1	33.4
Oxidized	C 1s	285.0	C-C,H	1.8	Nd
	As 3d5/2	45.2	As-O	1.8	100
	Ga 3d5/2	20.1	Ga-O	1.0	100

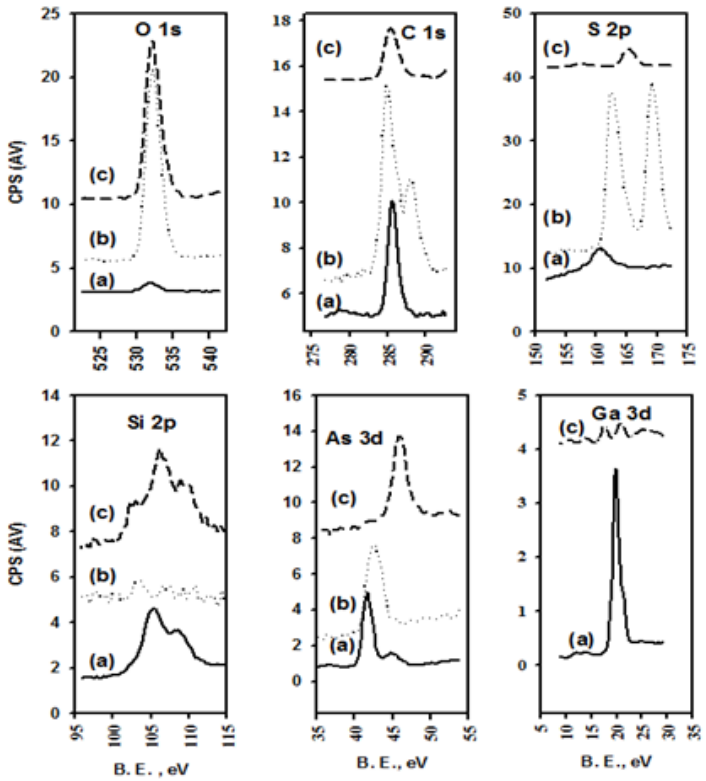

Figure 4. The detailed x-ray photoelectron spectra of a: (solid lines) fresh GaAs sample, b: (medium dashed lines) Sulfidized GaAs sample: sulfidation was made under potentiodynamic scanning for 150 scans from – 1 to + 1 V at 20 mV s^{-1} under illumination by light of intensity 25 mW cm^{-2}. The sulfidation path was composed of 0.8 MTU and 0.5 M H_2SO_4 and c: (dotted lines) Sample (b) was sputtered for 40 min. B. E. is the binding energy and AV is arbitrary values for the peak intensities.

XPS and high resolution XPS were used to characterize the surface composition and quantify the surface chemical bonding on different GaAs samples during sulfidation. Examples of XPS spectra are shown in Fig. 4 for a fresh, sulfidized and long-time sputtered GaAs samples. An example of high resolution XPS spectra for a sulfidized GaAs sample is also presented in Fig. 5. The bonds on sulfidized surfaces were composed of As – S, As – As, and S – O as well as some surface carbon bonds. From the data in Table 2, the oxidized GaAs sample exhibited only one As 3d doublet. All other samples had two As 3d doublets. The first doublet of the fresh and sulfuric acid treated GaAs appeared at 41.5 (As3d5/2); this is the normal binding energy value characterizing As – Ga bond [21, 31 – 34]. The second doublet at 44.5 eV is assigned as the As 2p3/2 line consisting mostly of oxide components with the core level chemical shifts of 3 eV corresponding to As_2O_3 [21 – 24]. The As 3d doublets for both sulfidized samples appeared in the range from ~ 41.5 eV to ~ 42.5 eV, likely represent As – Ga (41. eV), As – As (42 eV) and As(III) – S 42.5 eV [35 - 37]. The formation of the As – As bonding on the sulfidized samples, in the meantime, and the disappearance of the As – Ga bonding as seen from Table 2, are due to the generation of elemental As on the surface from the photoelectrochemical dissociation of GaAs as proposed in step 2 of the proposed reaction mechanism.

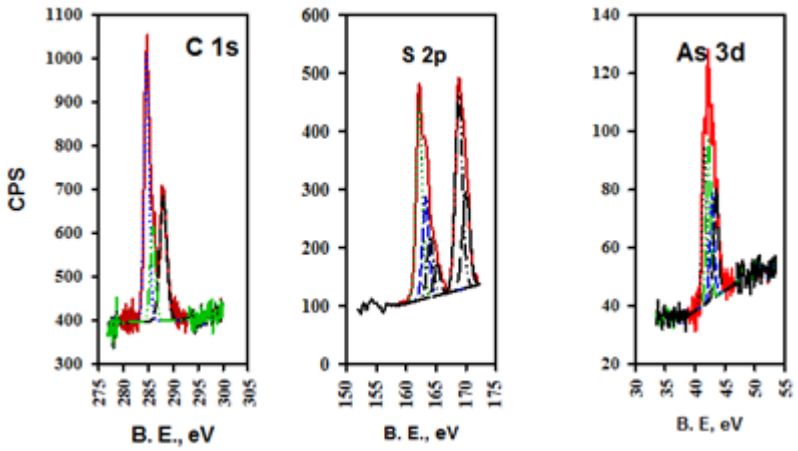

Figure 5. X-ray photoelectron spectroscopy high resolution peak fits of sulfidized GaAs sample: sulfidation was made under potentiodynamic scanning for 150 scans from −1 to+ 1 V at 20 mV s^{-1} under illumination by light of intensity 25 mW cm^{-2} The sulfidation bath was composed of 0.8 MTU and 0.5 M H_2SO_4.

Table 2 shows that long-time sulfidation resulted in further surface oxidation as implied from the formation of a high concentration of oxidized species like sulfide-As(III), sulfide-As(V) and As-As bonding. This Table also shows that the two sulfidized samples had two C 1s peaks at 288 and 285.7 eV which were assigned to the C=O and C-N bonds, respectively [38, 39]. The appearance of the C=O and C-N peaks was due to the adsorption of urea on the GaAs surface which was formed due to the dissociation of TU as suggested in step 5 of the above mechanism. Furthermore, the two sulfidized samples also exhibited strong S 2p peaks with three doublets. The three S 2p doubles appeared clearer in the high resolution spectra of Fig. 5. The first two doubles extended from 162.4 to

164.4; both were assigned to sulfur bonded to metals (As and/ or Ga) [31 – 34]. The spectral line appeared at 162.4 and 164.4 eV, consistent with S in the form of sulfide (S^{-2}), with one assigned to bonding to the trivalent As/ and or Ga (162.4 eV) and the other to the pentavalent As/ and or Ga (164.4 eV) [31 – 34]; supportive of steps 6 and 7 in the above mechanism. The third doublet at 169.1 eV was consistent with S^{+6} bonding, most probably SO_4^{-2} [34]; agreeing with step 8 of the proposed mechanism. Sulfate ions were formed due to the oxidation of sulfide ions during GaAs sulfidation. In order to exclude the possibility of interference between sulfates originated from sulfide oxidation and residual sulfate from electrolytes, an XPS spectrum for a GaAs sample treated only in 0.5 M H_2SO_4 was taken; its result is presented in Table 2. It is clear from this Table that sulfate formation is only associated with sulfidized GaAs samples, excluding the possibility of interference with residual sulfate from electrolytes.

The oxidation of sulfide to sulfate is an important result of this research. This oxidation step pumped out eight photogenerated holes from the GaAs surface, thereby partially inhibited GaAs corrosion.

Although XPS Ga peaks were clearly observed for the three electrodes that were not sulfidized, Table 2, no Ga peaks were found for the two sulfidized GaAs samples (notice the disappearance of the dotted line in the Ga spectra of Fig. 4). Moreover, the ICP-MS results in Fig. 3 consistently showed preferential dissolution of As ions. As seen in Table 2 the fresh GaAs had approximately equal surface As and Ga compositions. This pointed at the possibility that Ga ions diffused inward towards the bulk, while As atoms diffused outward towards the surface. Ga ion diffusion is expected to be very slow, but may be enhanced under the sulfidation experimental conditions. Indeed, the depth profiling experiments by prolonged Ar ions sputtering, which were carried out to test for As and Ga composition in deeper layers underneath the surface, strongly indicate that the Ga ions diffused towards the electrode bulk, Table 3.

Table 3. Atomic percentage of surface composition after different sputtering periods

Sputter time, min	C 1s	N 1s	O 1s	S 2p	As 3p	Ga 3d
10	39.3	18.4	24.5	14.4	3.4	nd
20	20.1	16.7	35.1	19.1	7.3	1.7
40	15.1	11.9	39.5	21.5	9.2	2.9

It was also noticed that after sputtering both As and Ga peaks were shifted towards higher binding energy values (notice the after sputtering As and Ga spectral lines of Fig. 4). Only one As 3d XPS peak could be seen at ~44.5 eV which was due to As – O bonds. Other peaks due to As – As, As – Ga, and As – S, were disappeared due to sputtering. This clearly indicates that sulfides were sputtered off the surface and left the surface covered with oxides. The formation of oxides underneath the surface indicates that the sulfide layer formed during the electrochemical sulfidation

was porous and did not prevent the aqueous electrolyte to penetrate and oxidize the bulk of the electrode. Deeper underneath the surface region where Ga became detectable after prolonged Ar ion sputtering, the Ga 3s (158 eV) peak was noticed to overlap with the S 2p (164 eV) peak. In order to adjust for this peak overlap, the area of the peak envelope as measured was assumed to be the sum of the areas of the overlapping peaks. The contributions from the Ga 3s and Ga 3p peaks were calculated by multiplying the measured area of the Ga 3d peak by the ratio of the relative sensitivity factors RSFGa 3s/RSFGa 3d and RSFGa 3p/RSFGa 3d. These contributions were then subtracted from the measured S 2p region area, and the difference was used as the accurate S 2p peak area listed in Table 3.

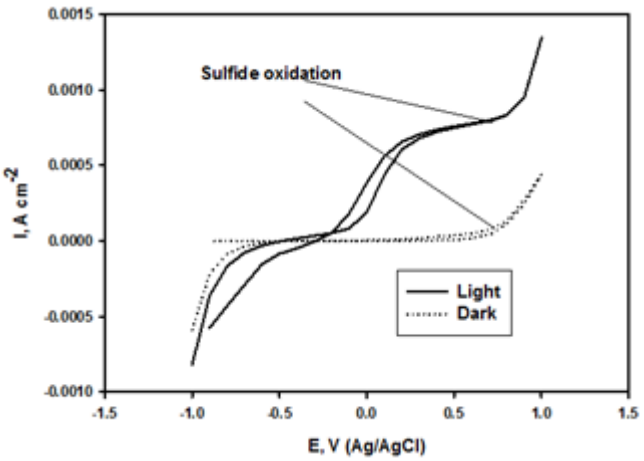

Figure 6. Current- voltage scans of GaAs after 50 scans at a rate of 20 mV s^{-1} in the dark and under illumination by 25mW cm^{-2} in 0.5 M H_2SO_4 and 0.8 M TU.

The oxidation of sulfide ions on GaAs surface has been further evidenced from the (I – E) curves presented in Fig. 6. Usually, the anodic photocurrents generated due to illuminating n-GaAs reach limiting values that depend solely on light intensity. However, for acidified TU electrolytes, after reaching an initial limiting value the photocurrent increased significantly at potentials more positive than 0.8 V. This increase was slight in the dark and pronounced under illumination as shown in Fig. 6. The observed increase in the anodic dark and photocurrents were higher after prolonged sulfidation due to the oxidation of the As-sulfide layer, which supports the above XPS results. It is thus expected that the oxidation of sulfide ions on GaAs surface pumped out some of the photogenerated holes from the surface. These positively charged carriers would have oxidized GaAs, and therefore we can conclude that oxidation of sulfides to sulfate suppressed GaAs oxidation.

4. CONCLUSIONS

Treatment of GaAs under illumination and potentiodynamic conditions in acidified TU electrolytes resulted in the formation of a smooth layer of As sulfide. Upon GaAs sulfidation, several

oxidation species such as As^0, As^{+3}, As^{+5}, S^{-2} and S^{+6} species were detected. The S^{+6} species ion was bound to oxygen, forming sulfate ions. The oxidation of S^{-2} to S^{+6} consumed eight photogenerated holes, and therefore competed with GaAs oxidation, resulting in a lower corrosion rate.

ACKNOWLEDGEMENT
This paper was made possible by a UREP 07 - 006 -1 – 002 from the Qatar National Research Fund (a member of Qatar Foundation). The statements made herein are solely the responsibility of the authors. The authors also wish to thank Professor Jan Kwak at the Chemistry & Earth Sciences Department, College of Arts & Sciences, Qatar University for valuable discussion and revising the manuscript.

References

1. T.V. L'vova, I.V. Sedova, V.P. Ulin, S.V. Sorokin, V.A. Solov'ev, A.A. Sitnikova, V.L. Berkovits and S.V. Ivanov, *Vacuum,* 57 (2000) 163.
2. V.L. Berkovits and D. Paget, *Appl Surf Sc*, 65 (1993) 607.
3. W. Jaegermann, R Rudolph, A Klein and C Pettenkofer, *Thin Solid Films*, 380 (2000) 276.
4. A. Etcheberry, H. Cachet, R. Cortes and M. Froment, *Surf Sci*, 472 (2001) 954.
5. H. Cachet, R. Cortès, M. Froment and A. Etcheberry, *Thin Solid Films*, 361 (2000) 84.
6. L. M. Depestel and K. Strubbe, *J Electroanal Chem,* 572, (2004)195.
7. D. V. Lioubtchenko, I. A. Markov and T. A. Briantseva, *Appl Surf Sci*, 211 (2003) 335.
8. M. S. Islam, P. J. McNally, D. C. Cameron and P. A. F. Herbert, *Thin Solid Films*, 290 (1996) 417.
9. V.L. Berkovits, *Appl. Surf. Sc.*, 65 (1993) 607.
10. S.T. Ali, S. Ghosh and D.N. Bose, *Appl Surf Sci*, 93 (1996) 37.
11. T. Tiedje, P. C. Wong, KAR Mitchell, W. Eberhardt, ZG Fu and D. Sondericker,, *Solid State Commun*, 70 (1989) 355.
12. L. Ferrari, M. Fodonipi, M. Righini and S. Selci, *Surf Sci*, 331 (1995) 447.
13. H. H. Huang, Z. Zou, X. Jiang and G. Q. Xu, *Surf Sci*, 396 (1998) 304.
14. A.S. Weling, K.K. Kamath and P.R. Vaya, *Thin Solid Films*, 215 (1992) 179.
15. J. Szuber, E. Bergignat, G. Hollinger, A. Polakowska and P. Koscielniak, *Vacuum,* 67 (2002) 53.
16. M. Oshima, T. Scimeca, Y. Watanabe, H. Oigawa and Y. Nannichi, *Jpn J Appl Phys*, 32 (1993) 518.
17. X.M. Ding, Z.L. Yuan, H.T. Hu, Z.S. Li, Y.F. Chen, X.Y. Chen, X.A. Cao, X.Y. Hou, Xwn Wang , E.D. Lu, S.H. Xu, P.S. Xu and X.Y. Zhang, *Nucl Instrum Methods B*, 133 (1997) 90.
18. K. Adlkofer and M. Tanaka, *Langmuir*, 17 (2001) 4267.
19. N. Nicoara, O. Custance, D. Granados, J. M. García, J. M. Gómez-Rodríguez, A. M. Baró and J. Méndez, *J Phys-Condens Mat,* 15 (2003) 2619.
20. FL S. Bhide and S. V. Bhoraskar, *J Appl Phys*, 72 (1992) 1464.
21. E.V. Konenkova, *Vacuum*, 67 (2002) 43.
22. C. C. Surdu-Bob, S. O. Saied and J. L. Sullivan, *Appl Surf Sci*, 183 (2001) 126.
23. I. Gérard, N. Simon and A. Etcheberry, *Appl Surf Sci*, 175 (2001) 734.
24. I. Gérard, C. Debiemme-Chouvy, J. Vigneron, F. Bellenger, S. Kostelitz and A. Etcheberry, *Surf Sci*, 433 (1999) 131.
25. M. M. Khader and A. S. Aljaber, *Appl Surf Sci*, 258 (2011) 68.
26. A.E. Bolza´n, R.C.V. Piatti and A.J. Arvia, *J Electroanal Chem*, 552 (2003) 19.
27. A.E. Bolzån, I.B. Wakenge 1, R.C. Salvarezza and A.J. Arvia, *J Electroanal Chem*, 475 (1999) 181.
28. M. Yan, K. Liu and Z. Jiang, *J Electroanal Chem.*, 408 (1996) 225.
29. M. Cui, M. Jang, S. Ibrahim , B. Park, E. Cho and J. Khim, *Ultrason Sonochem*, 21 (2014) 1527.

30. S. Tresintsi, K.Simeonidis, N.Pliatsikas, G.Vourlias, P.Patsalas and M.Mitrakas, *J Solid State Chem*, 213 (2014) 145.
31. S. Arabasz, E. Bergignat, G. Hollinger and J. Szuber, *Appl Surf Sci*, 252 (2006) 7659.
32. S. Arabasz, E. Bergignat, G. Hollinger and J. Szuber, *Vacuum*, 80 (2006) 888.
33. E. Godočíková, P. Baláž, Z. Bastl and L. Brabec, *Appl. Surf. Sci.*, 200 (2002) 36.
34. H. Yüzer, H. Doğan, J. Köroğlu and S. Kocakuşak, *Spectrochemica Acta B*, 55 (2000) 991.
35. A.B.M.O. Islam, K. Asai, K.K. Lim, T. Tambo and C. Tatsuyama, *Surf Sci*, 416 (1998) 295.
36. D.-Y. Choi, S. Madden, R.P. Wang, A. Rode, M. Krolikowska and B. Luther-Davies, *J Non-Cryst Solids*, 353 (2007) 953.
37. S. A. Wood and I. M. Samson, *Ore Geol Rev*, 28 (2006) 57.
38. A. Raab, S. H. Wright, M. Jaspars, A. A. Meharg, and J. Feldmann, *Angew Chem Int Edit*, 46 (2007) 2594.
39. M. Sc. Eda Jagst, *BAM Bundesanstalt für Materialforschung und –prüfung,* 2011, P. 34.